Nuclear Instruments and Methods in Physics Research A307 (1991) 504–511
North-Holland

High pressure xenon proportional counter up to 10 atm

H. Sakurai [1], B.D. Ramsey and M.C. Weisskopf
Space Science Laboratory, NASA Marshall Space Flight Center, Huntsville, AL 35812, USA

Received 29 January 1991

The characteristics of a conventional cylindrical geometry proportional counter filled with high pressure xenon gas up to 10 atm were investigated for use as a detector in hard X-ray astronomy. With a 2% methane gas mixture the energy resolutions at 10 atm were 9.8% and 7.3% for 22 and 60 keV X-rays, respectively. The corresponding resolutions at 1 atm were 7.7% and 5.1%. From calculations of the Townsend ionization coefficient it is shown that proportional counters at high pressure operate at weaker reduced electric field than low pressure counters. It is suggested that this is the fundamental reason for the degradation of resolution observed with increasing pressure.

1. Introduction

Xenon filled proportional counters are typically employed for medium-energy (< 100 keV) X-ray astronomy, but can be extended far beyond this point through operation at elevated fill gas pressures. If these pressures are sufficiently high, even a modest depth of gas can result in a significant efficiency. For instance, at 10 atm, 1 cm of gas will absorb around 10% of 100 keV photons.

The principal advantage of the proportional counter is its superior energy resolution over the solid scintillation counter which is usually employed as the conventional detector in hard X-ray astronomy. Generally, however, the energy resolution of proportional counters at high pressure is worse than at low pressure, particularly with xenon gas fillings where values of 10% FWHM at 10 atm and 6% FWHM at 1 atm have been reported for 60 keV X-rays [1].

There are many factors which could affect the energy resolution at high fill gas pressures. Foremost among these, for many practical systems, is contamination of the fill gas and/or the counter system. As will be discussed in more detail later, the reduced electric fields in the drift region away from the anode wire are much weaker at high pressure than at lower pressure, and hence the drift velocity of the primary electron cloud is lower at higher pressure. This in turn provides more opportunity for a loss of primary charge to electronegative impurities. The susceptibility of both xenon and argon based gas mixtures to such effects has been systematically investigated in ref. [2]. It was shown that xenon based gas mixtures are much more susceptible to electronegative impurities than argon based ones, and that methane quenched mixtures are comparatively less sensitive than with other quench gases. However, even with methane quenching, an impurity level of 10 ppm in xenon is serious for reduced fields of $\lesssim 0.1$ V/cm Torr.

In addition, there are other fundamental differences between operation at high and low pressures. Among these are the size of the primary electron cloud, and the strength of the reduced field in the avalanche region. The former could make the energy resolution at high pressures strongly dependent on the uniformity of the anode wire. The latter, through its effect on the Townsend ionization coefficient, modifies the energetics of the avalanche process and this in turn can result in changes in the statistical fluctuations which dominate the proportional counter energy resolution [3].

In order to investigate these problems, we have constructed a conventional cylindrical proportional counter and measured the gas gain and the energy resolution at a range of pressures between 1 and 10 atm for both pure xenon gas and xenon + methane mixtures.

2. Apparatus

The detector used for the investigation was a conventional rectangular geometry proportional counter having a cross section of 1 cm × 1 cm and a length of 4 cm along the anode wire. The counter was made of stainless steel and the entrance window, which was a 250 μm thick aluminum sheet sealed with indium on one side,

[1] NAS/NRC Senior Resident Research Associate on leave from Yamagata University, Yamagata, Japan.

formed one of the four cathodes. The anode wire, of diameter 25 μm, was soldered into feedthroughs welded in the counter at both ends and positioned in the geometric center of the cathodes to an accuracy of 50 μm. The ceramic insulated feedthroughs were potted with silicon elastomer on the outside of the counter to prevent discharge in air.

The evacuation and gas filling system, including an Oxysorb purifier, consists of all stainless tubes and bellows valves which are rated up to 70 atm. The fill gas pressure was measured to an accuracy of 1 Torr using a capacitance manometer. Before filling, the counter and the gas filling lines were baked at a temperature of 70 °C for three days. After bakeout the outgassing rate of the counter was less than 10^{-8} Torr/s. We used fresh xenon and methane gases of research grade purity. There was no discernible difference in energy resolution with and without the purifier at 1 atm fill gas pressure, but the purifier was used for all measurements at high pressure.

The signal from the detector was routed through a low noise, charge-sensitive preamplifier, Ortec/EG & G model 142PC, to a main amplifier, Ortec 410. Tests with various shaping time constants showed no noticable difference in energy resolution for gas mixtures having normal drift velocities. So, typically, shaping time constants of 1 μs differentiation and 2 μs integration were used.

The gas gain and the energy resolution were measured using collimated ^{109}Cd (22 keV) and ^{241}Am (60 keV) sources. The gas gain was derived by measuring the peak amplitude of the preamplifier output pulse on a calibrated oscilloscope and then employing a conversion factor, previously derived from a calibrated charge input, of 6.78 V/pC. A mean ionization energy of 21 eV was used for both pure xenon and xenon + methane. The overall error in this procedure, factoring in measurement errors which are greatest at the lowest gas gains, is estimated to be at maximum ±7%.

3. Results and discussion

3.1. Contamination

A calibration of the cleanliness of the counter and the fill gas was carried out by adding oxygen as an impurity to pure xenon. The energy resolutions at 22 keV for three pure xenon gases from different bottles, and pure xenon gas with the addition of various levels of oxygen up to 33 ppm, are shown as a function of gas gain at 10 atm in fig. 1. Also, the energy resolutions at gas gains of 50 and 600 are shown, as a function of the concentration of oxygen in pure xenon at 10 atm, in fig. 2. These figures show that: 1) the energy resolutions of the pure xenon gases are almost constant and independent of gas gain at around 10%; 2) even a modest amount of contamination can seriously degrade the energy resolution at high pressure, as in fig. 2 where 3 ppm of oxygen lowers the energy resolution to 13% at a gain 50; and 3) under contamination conditions the energy resolution in general degrades as the gas gain is reduced. Further, as shown in fig. 3, at 5 atm the degradation of the energy resolution due to impurities is much smaller than at 10 atm, there being no discernible difference in energy resolution between the pure xenon gas and the xenon gas with an impurity level of 16 ppm.

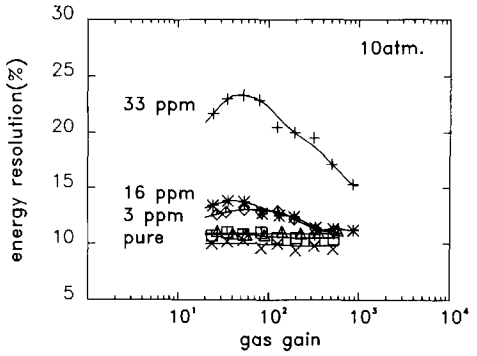

Fig. 1. Measured energy resolution at 22 keV for pure xenon gases, and xenon with oxygen added as an impurity, as a function of gas gain at 10 atm. The hand-drawn smooth lines are only intended to guide the eye. The energy resolutions at gas gains less than 60 are with noise subtracted.

As the estimated reduced fields at the wall of the counter, over the range of gas gains shown, are between 0.09 and 0.11 V/cm Torr at 10 atm, and between 0.14 and 0.17 V/cm Torr at 5 atm, the results indicate that pure xenon gas is very susceptible to contamination with impurities such as oxygen at reduced fields of less than 0.13 V/cm Torr and hence at high pressure.

The fact that we obtain the same energy resolution for three different sources of pure xenon gas, each of which is certified less than 1 ppm of oxygen, coupled with the lack of dependence of energy resolution on gas

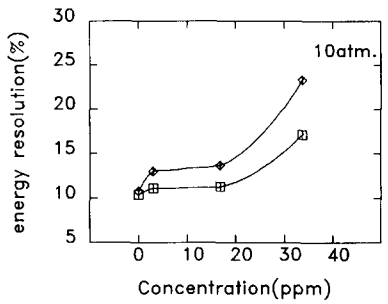

Fig. 2. The dependence of the energy resolution on the concentration of oxygen in xenon gas for gains of 50 (◇) and 600 □). The hand-drawn smooth lines are only intended to guide the eye.

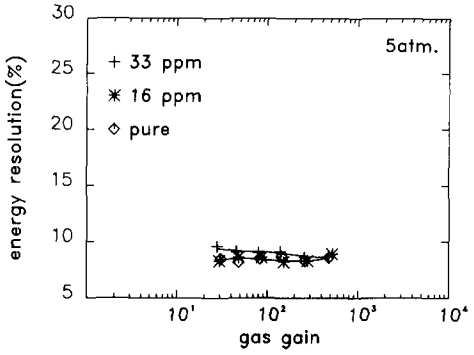

Fig. 3. Measured energy resolution at 22 keV for pure xenon gas, and xenon plus oxygen added as an impurity, as a function of gas gain at 5 atm. The hand-drawn smooth lines are only intended to guide the eye. The energy resolutions at gas gains less than 60 are with noise subtracted.

gain for the pure gas fill, and the large changes when small quantities of oxygen are added, all lead us to conclude that the detector, the gas fill system and the gas itself are indeed free from contamination to better than 1 ppm.

3.2. Gas gain

Fig. 4 shows the gas gain as a function of applied voltage for pure xenon gas and xenon + 2% methane at a range of gas pressures from 1 to 10 atm. The voltage is seen to increase much more slowly than the pressure, being roughly a factor of 3 for a 10-fold increase in pressure. Also, the slope of the voltage vs gain curves seems to decrease as the fill gas pressure increases. This is a consequence of the relationship between the Townsend ionization coefficient, the gas pressure, and the electric field.

The Townsend ionization coefficient α can be represented by the semi-empirical formula

$$\alpha = Ap \exp[-B/(E/p)],$$

where E is the electric field, p is gas pressure and the constants A and B depend on the gas filling.

The gas gain of a cylindrical proportional counter, which is the integral of the Townsend ionization coefficient from the anode surface to the cathode, is given by

$$G = \exp((A/B)V \exp[-Bpr_a/V]),$$

where $V = V_0/\ln(r_c/r_a)$, V_0 is the applied voltage between anode and cathode, and r_a and r_c are the anode wire radius and the cathode tube radius [4].

The constants A and B can be derived from the gas gain vs voltage data at each pressure and these in turn can be used to generate the corresponding Townsend ionization coefficient as function of field. These data are shown in a fig. 5 along with corresponding data from Kruithof [5]. The data clearly show that the ionization coefficient is represented by one curve for pressures between 1 and 10 atm, and that the multiplication of electrons at higher pressure is carried out in regions of lower reduced electric field.

Simply, to ionize a molecule of ionization potential V_i in an electric field E an electron would be required to travel a characteristic distance $l \geq V_i/E$. The probability of an electron traveling the distance between l and $l + dl$, that is the probability of an ionizing collision, is $(1/\lambda) \exp[-(l/\lambda)]\, dl$ for a collision mean free path λ [6]. As $\lambda = \lambda_0/p$, to get the same gas gain at high pressure p (p expressed in atm), as at 1 atm, the characteristic distance at pressure p would be $l_p = (l_0 + \lambda_0 \ln p)/p$, where l_0 and λ_0 are the characteristic distance and the collision mean free path at 1 atm. So,

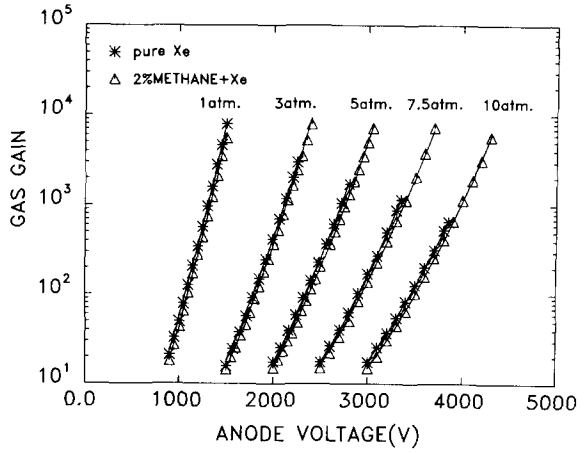

Fig. 4. Gas gain as a function of anode voltage at each pressure between 1 and 10 atm for pure xenon and 2% methane gas mixture. The solid lines are best fit curves obtained with a least squares method.

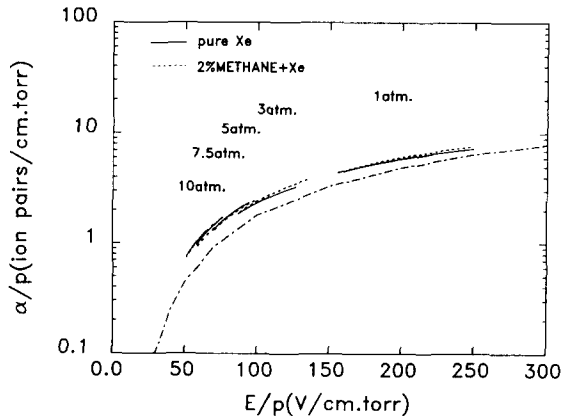

Fig. 5. Townsend ionization coefficient α/p as a function of reduced field, calculated from the gas gain at each pressure. The dot-dash line is the measurement of Kruithof [5] (see text).

the field necessary for ionization then is given by $E \geq pV_i/(l_0 + \lambda_0 \ln p)$ and hence the voltage increases much more slowly than pressure. Further, for a given absolute change in applied voltage, the reduced field $\Delta(E/p)$ at high pressure increases more slowly than at low pressure and hence the increase of gas gain is more gentle. Also, using this notation, the Townsend ionization coefficient is described as $(p/\lambda_0) \exp[-(V_i/\lambda_0)/(E/p)]$, so A and B correspond to $1/\lambda_0$ and V_i/λ_0, respectively and hence $B/A = V_i$.

Fig. 6 shows the Townsend ionization coefficient α in pure xenon at a gas gain of 100 for each gas pressure between 1 and 10 atm. This suggests that at higher pressure the avalanche begins closer to the anode, because the gas gain is the integral of α over the distance to the anode. The region of the avalanche is estimated to be 35 μm at 1 atm and 20 μm at 10 atm, as derived from the constants A and B. Kruithof measured the Townsend ionization coefficient for xenon gas by measuring the current between two parallel electrodes at low pressure (< 200 Torr). Our result is slightly greater as shown in fig. 5. In fig. 7 the values B/A, which should be the ionization potential of the xenon atom, $V_i = 12.1$ V, are plotted at each pressure. The Kruithof data were scaled according to pressure. The Kruithof data show a gradual increase in the value B/A with decreasing reduced field, but our results are approximately constant. Why these two experimental techniques differ is still not well understood.

Whilst the methane quenched gas fills operated stably at gas gains up to 10^4, regardless of pressure, the same was not true for pure xenon which would break down below this point for fills above 1 atm. The onset of breakdown in pure xenon occurred at progressively lower gas gains, as the pressure was increased, as is evident from fig. 4. Usually, breakdown is caused by the liberation of electrons from the cathode walls under the impact of positive ions and/or photons from the xenon gas. If the breakdown were due to the positive ions, the gas gain at which the breakdown begins would be similar for each pressure. We must conclude therefore that the breakdown is mainly due to photons generated

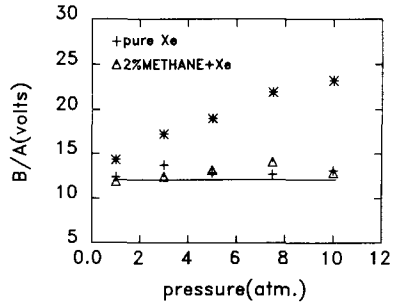

Fig. 7. The ratio of B to A, which are constants in the semi-empirical formula of the Townsend ionization constant, obtained from gas gain measurements at each pressure. The asterisks are the ratio calculated from the data of Kruithof at the reduced field correspond to each pressure. The ratio is a measure of the ionization potential of the fill gas atom (see text).

from the excitation of the xenon gas in the avalanche and that this excitation increases with pressure. Fig. 8 shows the dependence of the inverse gas gain, at which breakdown occurs, on pressures between 3 and 10 atm. This suggests that the excitation of the xenon gas increases exponentially with pressure in the cylindrical proportional counter. With the addition of methane quench gas the mixture is stabilized, possibly due to collisional deexcitation of the xenon atoms by methane molecules. Direct photoabsorption is unlikely as the absorption band of methane is not well matched to the xenon emission spectrum [7].

3.3. Energy resolution

In figs. 9 and 10 the energy resolutions at 22 and 60 keV, respectively, are shown as a function of gas gain for each pressure of the xenon + 2% methane mixtures. At a gain of about 100, the energy resolutions were 7.7% and 9.8% for 22 keV, and 5.1% and 7.3% for 60 keV at 1 and 10 atm, respectively. These data indicate that at each pressure the dependence of the energy resolution on the gas gain is approximately the same, and that the

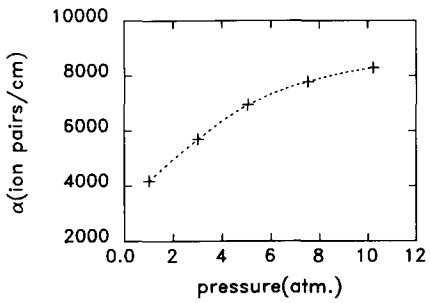

Fig. 6. Townsend ionization coefficient α at a gas gain of 100 for each pressure in pure xenon fill gas.

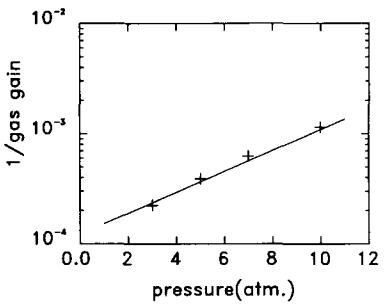

Fig. 8. The inverse of gas gain at breakdown for pure xenon at each pressure. The solid line is the best fit to the data.

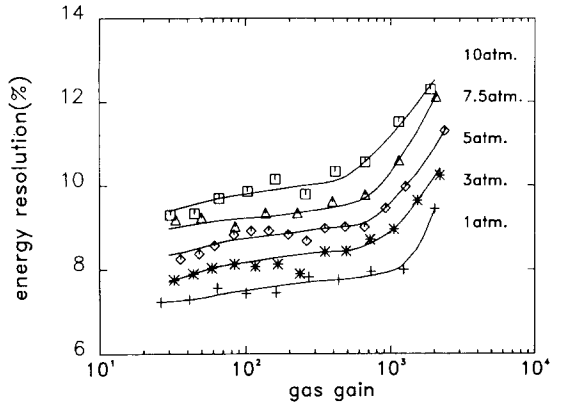

Fig. 9. Measured energy resolution of 2% methane quenching as a function of gas gain at 22 keV for each pressure between 1 and 10 atm. The hand-drawn smooth lines are only intended to guide the eye. The energy resolutions at gas gains less than 60 are with noise subtracted.

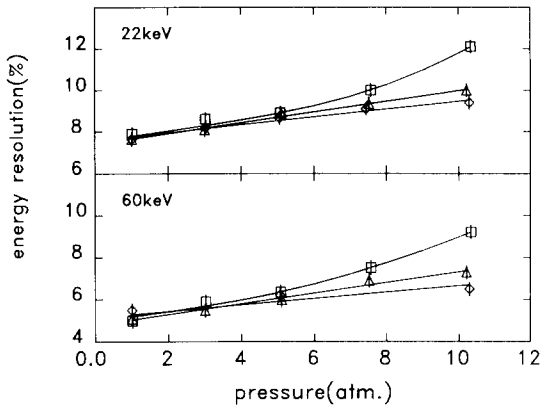

Fig. 11. The dependence of the energy resolution on pressure for pure xenon (◇), 2% methane (△) and 5% methane (□) gas mixtures. The gas gains are 250 and 100 for 22 and 60 keV, respectively.

energy resolution degrades with increasing pressure. Also, the energy resolutions begin to deteriorate very rapidly above gains of 800 and 300 for 22 and 60 keV X-rays, respectively. This indicates that, when the total charge after multiplication is over 8.5×10^5 electrons, the energy resolution degrades regardless of the initial amount of the primary charge, presumably due to space charge effects.

Fig. 11 shows the energy resolutions as a function of pressure for pure xenon, xenon + 2% methane and xenon + 5% methane gas mixtures at gas gains around 250 and 100 for 22 and 60 keV X-rays, respectively. The rate of increase of the energy resolution for pressures from 1 to 10 atm was quite similar for the pure xenon and xenon + 2% methane, but for the 5% methane gas mixture the energy resolution at 10 atm was significantly worse.

One possible source of fluctuations in energy resolution would be contamination of the gas resulting in a loss of primary charge on the way to the avalanche region. As shown in section 3.1, pure xenon gas at high pressure is very much more susceptible to small amounts of impurity, but we concluded that the impurity level was less than 1 ppm for the pure xenon gases used in the measurement. Also, as shown in fig. 11, the slopes of the energy resolution of the pure xenon and the xenon + 2% methane mixture are a gradual linear function of pressure. This change in resolution with pressure cannot be due to impurities at the ppm level as we have already seen that 5 atm fill gas pressure the addition of 16 ppm of oxygen had no discernible effect on the energy resolution. Further, since the drift velocity of electrons in pure xenon gas is much smaller than for gas mixtures of methane and xenon [8], the effect of gas contamination for pure xenon gas should be much stronger than methane plus xenon, but the measured data indicate the opposite behaviour. For these reasons and from our own original check of the gas quality we can therefore rule out gas contamination as the major cause of energy resolution dependence on pressure.

Fig. 12 shows the pulse height distributions for 22 keV X-rays illuminated on two different points of an anode wire at pressures of 1, 5 and 10 atm of pure xenon fill gas. Point A, which represents typical wire uniformity, gives energy resolutions of 7.6% to 9.7% at pressures from 1 to 10 atm. Point B, on the other hand, is a portion of wire with a high degree of nonuniformity and gives corresponding resolutions of 7.8% to 19.3%. The difference in the fluctuation between points A and B, is shown in fig. 13 at pressures of 3 to 10 atm,

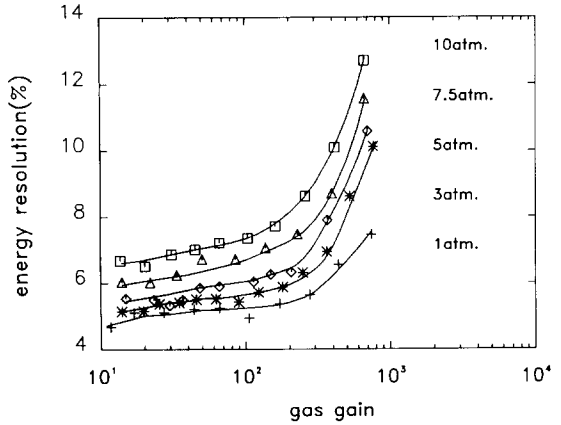

Fig. 10. Measured energy resolution of 2% methane quenching as a function of gas gain at 60 keV for each pressure between 1 and 10 atm. The hand-drawn smooth lines are only intended to guide the eye. The energy resolutions at gas gains less than 30 are with noise subtracted.

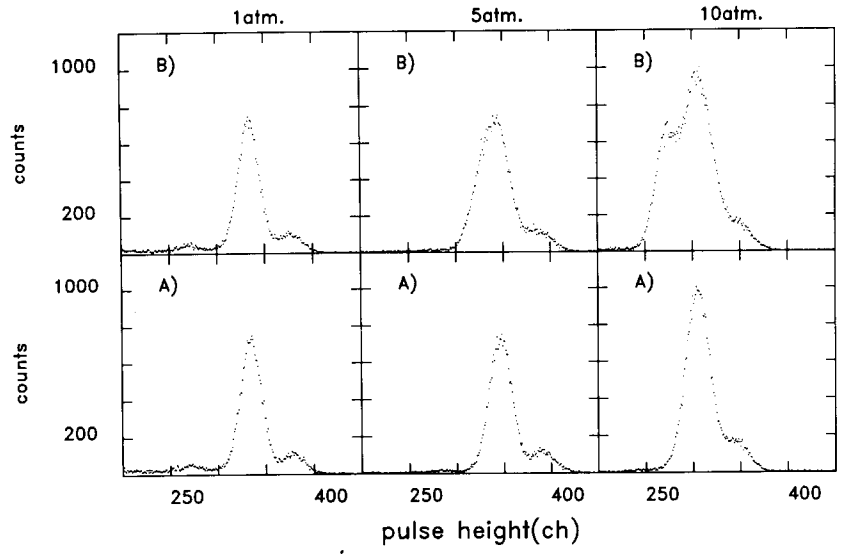

Fig. 12. The pulse height distributions for 22 keV X-rays illuminated on two points, A and B, of an anode wire at pressures of 1, 5 and 10 atm.

indicating approximately a function of pressure with power of index 1.

To understand how this relationship arises consider that, as the fill gas pressure is increased, the range of the primary photoelectron decreases and hence the initial charge cloud becomes smaller. Also, diffusion of the resulting electron cloud affects its size in proportion to $1/\sqrt{p}$, where p is the pressure. So, the average size of the electron cloud is $\sqrt{s^2 + 2Dtp}/p$, where s is the size of the primary electron cloud, D the diffusion constant at 1 atm, and the t is the drift time. Hence the average size of the cloud is approximately an inverse function of pressure.

From the published data on the range [9,10] and the diffusion coefficient [8,11] of electrons in xenon gas, the estimated sizes of the electron clouds for 22 keV X-rays are 1.5 mm and 170 μm for typical 3.5 mm drift in pure xenon gas at pressures of 1 and 10 atm, respectively. If the electron cloud comes to the anode wire surface from a point say 3.5 mm (a typical distance) from the anode along the electric field lines, then the sizes when projected to the anode wire surface will be about 5 and 0.6 μm at 1 and 10 atm, without considering broadening of the electron cloud in the avalanche.

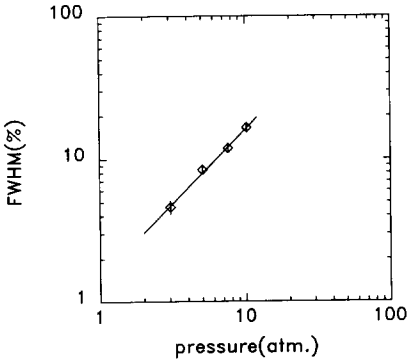

Fig. 13. The dependence of the difference in the energy resolution between points A and B on pressures between 3 and 10 atm. The solid line is a best fit to the data.

So, obviously, the dependence of the energy resolution on the uniformity of the anode wire surface would be much more sensitive at higher pressure. The effect would also be more significant for methane gas mixtures at higher pressure than for pure xenon gas, because of the smaller diffusion coefficient in quenched mixtures. Thus it may be possible to explain the difference of the energy resolution at high pressure between the pure xenon and the 2% methane gas mixture. It is difficult, however, to explain the difference of the energy resolution at higher pressure between 2% and 5% methane gas mixture in the same way.

The fluctuation in the pulse amplitude from a proportional counter is the sum of the primary fluctuations, which depend on the number of charges generated by the incoming X-ray, and the fluctuations in the multiplication process. The energy resolution of the proportional counter is given by $\sqrt{(F+f)W/E}$, where E is the energy of the X-ray, W is the mean ionization energy for the gas mixture, F is Fano factor, and f is the variance of gas multiplication for one electron [11]. From the theoretical considerations of Alkhazov [3], for multiplication due to ionization, f depends on the quantity $\chi = \alpha V_i/E$, which is the ratio of the characteristic distance V_i/E to the mean free path of the ionization $1/\alpha$, and hence the pressure because of the pres-

sure dependence of the Townsend ionization coefficient as shown in section 3.2. The deviation of the probability distribution of the number of electrons in the avalanche is smaller when the ratio is greater. Fig. 14 is the variation, with fill gas pressure, of this ratio calculated at the point from the anode at which the multiplication has a value of 2, and for a final gas gain of 100. This position represents the first step in the avalanche chain, and is derived using the Townsend ionization coefficient obtained from the gas gain curves. Fig. 14 shows that the ratio is smaller at higher pressure.

Although the energy of an electron in the avalanche region goes into both ionization and excitation of the gas atom, at strong reduced field the ionization will be dominant, while at weak field, on the contrary, the excitation will be comparable to the ionization. Also, the variance in the avalanche size will be controlled by fluctuations at the very beginning of the multiplication region. In the cylindrical proportional counter, the estimated reduced fields at which an electron is initially multiplied to two electrons, are 73 V/cm Torr at 1 atm and 34 V/cm Torr at 10 atm for a gain of 100 in pure fill gas. So, at high pressure, comparatively more energy will be spent on excitation than ionization and hence the value of ratio χ will decrease.

It is interesting to compare the dependence of energy resolution on pressure of methane and xenon with ones derived from methane and argon [12]. The pressure dependence found by these workers is very similar to our results, but the mechanisms discussed, in particular a photon emission–absorption channel for producing the initial charge cloud, necessitate a large dependence of the mean ionization energy on pressure, and an energy transfer mechanism which is energetically impossible in xenon + methane. (Note that the W values of argon are constant at pressures of 0.2 and 2 atm [13,14].)

As noted earlier, as the fill gas pressure is raised, an increasing amount of energy in the avalanche goes into excitation compared with ionization. For pure xenon the channel $Xe^* + Xe \rightarrow Xe_2^+ + e$ is possible [15] converting some of this excitation into ionization, but for the methane quenched gas mixture the energy of the excited xenon would be transferred to the methane molecule by collision with no additional ionization resulting. Thus the avalanche fluctuations would be greater in the methane mixture than the pure xenon and hence the energy resolution would be inferior. The collision rate for the methane mixture will increase with the concentration of methane molecules. So, the avalanche fluctuations and hence the energy resolution of the methane gas mixtures would be greater at large quench gas concentrations.

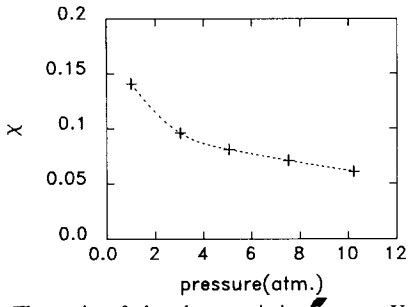

Fig. 14. The ratio of the characteristic distance V_i/E to the mean free path for the ionization at each pressure (see text).

4. Conclusion

We have presented results on the performance of a high pressure cylindrical proportional counter filled with pure xenon gas and xenon + methane gas mixtures up to 10 atm.

By utilizing an ultraclean system we have avoided the contamination effects which usually plague high pressure xenon work. This has permitted an investigation into changes with pressure on a more fundamental level.

Through an analysis of the Townsend first ionization coefficient, it was shown that proportional counters at high pressures operate at a weaker reduced field. This results in an increase in excitation relative to ionization and this in turn results in greater avalanche fluctuations and inferior energy resolution. The key here is the ratio of the characteristic distance (V_i/E) to the ionization mean free path ($1/\alpha$). As this ratio increases, more energy is channeled into ionization than excitation, and the avalanche fluctuations decrease.

It was also shown that for some mixtures wire nonuniformity becomes a problem as the fill gas pressure is increased. Overall, though, the energy resolution for pure xenon and xenon + 2% methane fill gases increased by approximately 2% when the fill gas pressure was increased from 1 to 10 atm.

It is interesting to compare the behaviour of the cylindrical proportional counter at high pressure with the parallel grid proportional counter at low pressure, as they both have similar reduced field. This work is currently in progress and will be followed by more detailed investigations of the parallel geometry with xenon plus methane and other quench gases such as isobutylene and trimethylamine.

References

[1] R.K. Sood, R.K. Manchanda and Z. Ye, 28th Cospar Meeting, 1990.

[2] B.D. Ramsey, R.F. Elsner and M.C. Weisskopf, Nucl. Instr. and Meth. A270 (1988) 178.

[3] G.D. Alkhazov, Nucl. Instr. and Meth. 89 (1970) 155.
[4] G.D. Alkhazov, Nucl. Instr. and Meth. 75 (1969) 161.
[5] A.A. Kruithof, Physica 7 (1940) 519.
[6] A. von Engel, Handbuch der Physik XXI (1956) 504.
[7] G.L. Weissler, Handbuch der Physik XXI (1956) 304.
[8] A. Peisert and F. Sauli, Drift and Diffusion in Gases: A Compilation, CERN 84-08 (1984).
[9] M.J. Berger and S.M. Seltzer, Tables of Energy Losses and Ranges of Electrons and Positrons, NASA SP-3012 (1964).
[10] J.E. Bateman, M.W. Waters and R.E. Jones, Rutherford Lab. Report RL-75-140 (1975).
[11] H. Sipilä, Nucl. Instr. and Meth. 133 (1976) 251.
[12] R.K. Manchanda, Z. Ye and R.K. Sood, Nucl. Instr. and Meth. A292 (1990) 373.
[13] W.P. Jesse, Phys. Rev. 174 (1968) 173.
[14] S. Sasaki, M. Miyajima, K. Katoh, M. Takabe and K. Seto, KEK report 84-17 (1984).
[15] J.A. Hornbeck and J.P. Molnar, Phys. Rev. 84 (1951) 621.